

The Applicability of Temperature Correction to Chemoresistive Sensors in an e-NOSE-ANN System¹

Rosalyn Hobson^{†¶} and Anthony Guiseppi-Elie^{‡¶}

[†]Department of Electrical Engineering [rshobson@vcu.edu], [‡]Department of Chemical Engineering [guiseppi@vcu.edu], and [¶]Center for Bioelectronics, Biosensors and Biochips (C3B), Virginia Commonwealth University, P.O. Box 843028, Richmond, Virginia 23284-3028, USA

ABSTRACT

The influence of the temperature sensitivity of chemoresistive, inherently-conductive-polymer (ICP) sensors on the performance of an artificial neural network (ANN) e-NOSE system is evaluated. Temperature was found to strongly influence the responses of the chemoresistors. An e-NOSE array of eight ICP sensor elements, a relative humidity (RH) sensor and a resistance temperature device (RTD) was tested at five different RH levels while the temperature was allowed to vary naturally. A temperature correction algorithm based on the temperature coefficient of resistance, β , for each material was independently determined and applied to raw sensor data prior to input to the ANN. Conversely, uncorrected data was passed to the ANN. The performance of the ANN was evaluated by determining the error found between the actual humidity versus the calculated humidity. The error obtained using raw input data was 10.5% and using temperature corrected data 9.3%. This negligible difference demonstrates that the ANN was capable of adequately addressing the temperature dependence of the chemoresistive sensors.

Keywords: e-NOSE, ANN, chemoresistive sensors, temperature dependence.

1 INTRODUCTION

The fundamental principles of biological olfaction, such as nature's use of arrays of semi-selective sensors and sophisticated pattern recognition², have become the basis for a whole new generation of analytical instrumentation called e-NOSES³. Inspired by nature, these instruments are fully capable of vapor-phase chemical detection and quantification⁴. In our laboratories we have developed prototype instrumentation which serves as a test-bed that is capable of chemical detection and quantification. The sensor system comprises an array of chemoresistive sensor elements that are formed from inherently conductive polymers, a multi-element interrogation protocol, real-time data acquisition and reduction, integrated pattern recognition and pattern visualization, and a pattern recognition neural network to remove inter and intra-observer bias in the interpretation of patterns. This system

can potentially be used to provide low cost unattended monitoring of volatile organic compounds (VOCs) implicated in environmental emissions and occupational health, as well as for the monitoring of the ambient by individuals suffering olfactory impairment.

2 BACKGROUND

E-NOSES based on the use of inherently conductive polymers as chemoresistive devices have been previously described⁵. Some have even been successfully commercialized⁶. One major consideration in the use of ICPs as e-NOSE sensory devices is the tremendous temperature-dependent sensitivity of the resistance⁷.

2.1 The Sensor Array

The sensory elements are chemoresistive devices comprising a thin film of an inherently conductive material dispersed in a VOC-swellable polymer matrix and deposited onto a microlithographically fabricated interdigitated array. Each element was made from commercially available microlithographically fabricated interdigitated microsensor electrodes (IMEs) shown in Fig. 1. Each IME chip (1.0 cm x 2.0 cm x 0.05 cm) of magnetron sputtered gold on boroasilicate glass forms a sensory or transducing element of the sensor array. Eight such devices comprise an 8-element array. Each element is rendered VOC sensitive by coating of the interdigit region with a thin film of a unique, VOC-sensitive inherently conductive polymer. The metallization pattern on the chip creates an interdigit region comprised of 50 digits on each bus. Each digit and adjacent space measured 10 μ m. These regions of interdigitation were each coated with inherently conductive polymer such that a chemoresistive sensor device was the result.

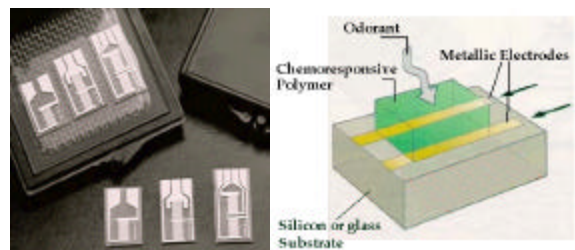


Figure 1: Microfabricated interdigitated microsensor chip (L) and chemoresistive sensor device (R).

The chemoresistive materials of the sensors were: spun-cast chemically synthesized polyaniline at two film thickness levels, electropolymerized polypyrrole of two different counteranion formulations, electropolymerized poly-3-methyl thiophene at two film thickness levels, and single-walled carbon nanotubes dispersed in polydimethylsiloxane (two different formulations). These were combined with a RTD ($\pm 0.1^\circ\text{C}$) and a RH sensor (0.1% RH). These ICP materials are nonspecific and typically yield conductimetric responses to a wide variety of gas and vapor molecules. The precise response of a sensor element varies as the concentration and type of gas/vapor molecule changes. By using multiple IME sensing elements, it is possible to generate a unique signal for vast numbers of compounds; furthermore the signal will identify not only the species present but also its concentration.

2.2 ANNs and e-NOSE

Electronic noses that use ANNs for data analysis have been demonstrated in various applications⁸. Using an ANN in conjunction with a sensor array has been shown to increase the number of detectable chemicals. The types of ANN architectures typically used in this application can be divided into two categories, recurrent and feedforward. The recurrent architecture uses state feedback information to aid in the analysis of time dependent data. In the feedforward architecture all information is propagated forward through the network.

The types of training can be divided into supervised and unsupervised training. Supervised training uses a pattern classifier to relate specific sensor outputs to specific compounds. Learning occurs when the ANN is presented with sensor outputs (or measured attributes) and compound labels. During training, using these input-output training pairs, the ANN learns to correlate the sensor output to specific compounds. Supervised algorithms used in electronic noses include backpropagation, learning vector quantizer, and fuzzy ARTmaps⁹. Unsupervised learning does not require predetermined compound classes for training. It performs a clustering of the data into similar groups based upon the measured attributes or features that serve as inputs to the ANN. Unsupervised algorithms used in e-NOSEs include self-organizing maps and adaptive resonant theory networks¹⁰.

In this work a high-speed workstation digitized and stored the data from the sensor array and ran ANN used to analyze the data. A three layer feedforward ANN (Fig. 2) was used for data analysis, with the input layer consisting of 6, the hidden layer 13, and the output layer 5 processing elements (PE). Each PE in the input layer received outputs from each sensor. Each PE in the output layer was sensitive to a specific challenge level of the candidate vapor. The ANN was trained using a backpropagation algorithm. The input to the ANN was a ten element input vector consisting of the sensor responses, temperature and relative humidity.

The output of the ANN was a five-element output vector where each parameter represented a specific relative humidity.

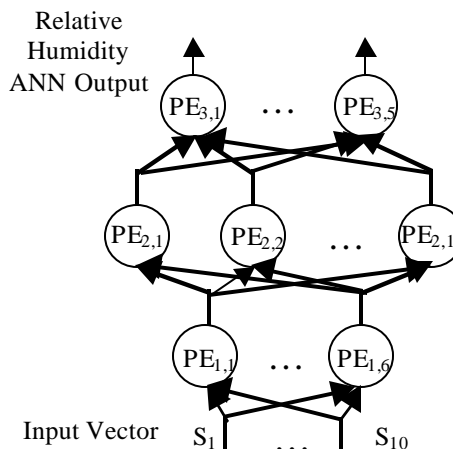


Figure 2. Feedforward ANN architecture.

2.3 Temperature dependence and e-NOSE

Exposure of the polymer film to vapor leads to a measurable change in the electrical impedance (resistance) as the polymer matrix swells and the conductive filaments are separated. However, temperature is also known to strongly influence the conductivity of these materials⁷. Over small spans of absolute temperature (T) there is an approximate linear relationship of the form $\ln(R_T) = A + (\beta/T)$ where β is a materials constant of the temperature responsive material. For a resistance $R_T(T)$ and $R_{T_0}(T_0)$ at a reference temperature, T_0 , one obtains:

$$R_T \cong R_{T_0} \exp \left[\frac{\beta(T_0 - T)}{T T_0} \right] \quad (1)$$

The temperature coefficient of resistance, β , can thus be approximated from the slope of the line $\ln(R_T)$ vs. $1/T$ (Fig.3).

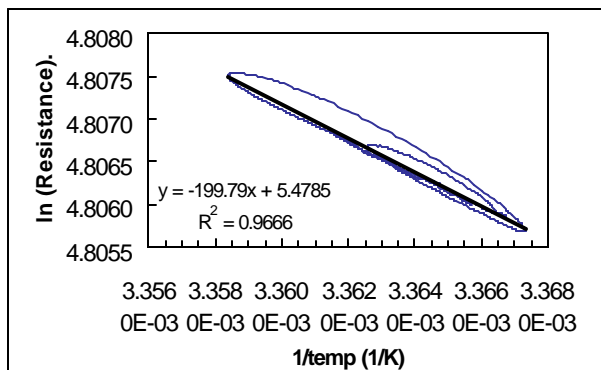


Figure 3. Typical plot for determination of the temperature coefficient of resistance, β .

3 EXPERIMENTAL

The e-NOSE test bed is designed to automate and regulate the process of gathering experimental data from the e-NOSE array of chemoresistive sensor elements. It consists of a gas/vapor manifold subsystem, an instrumentation control and data acquisition subsystem, and data analysis and display software. Two input/output interface cards: a Computer Boards CIO-DAS08Jr/16-AO and a National Instruments GPIB card were used to control and regulate gas/vapor flow through the manifold subsystem and for instrument control and data acquisition from a Model 2010/Model 2000 Multimeter/Multiplexer (Keithley, Chicago, IL) respectively.

Three separately controllable Mass-Flow Controllers (MFP 100, 10, 1 scc/min, Cole-Palmer, Vernon Hills, IL) and electronically actuatable solenoid valves regulated the flow of a pure carrier gas stream of purified dry nitrogen over the array. A bypass stream comprising a fraction of the gas flow was bubbled through a reservoir of DI water held at constant temperature. Heating and cooling of the reservoir was provided by a compact, solid state thermoelectric stage (Melcor Corp., Trenton, NJ). By maintaining a constant flow rate of 20 scc and selectively varying the ratio of pure carrier gas to vapor-containing stream, a wide range of RH vapor streams could be presented to the array. The data acquisition and instrument control software was written in TestPoint (Capital Equipment Corporation, Billerica, MA). Raw resistance data was streamed to MS Excel, normalized ($R_N = (R_t - R_0)/R_0$) and plotted versus time.

Exposure tests were performed by varying the percentage of the 100 % RH vapor stream that was blended into the pure carrier gas stream. In this way RH values of 10, 20, 30, 40 and 50% were studied. Temperature dependence of the responses of the individual elements of the sensor array was measured under constant RH conditions. The expose pattern typically comprised a two-phase exposure cycle within which the first was a 30-min. phase of exposure to pure carrier gas. This was followed by a 30-min phase of exposure to the appropriate level of RH.

4 RESULTS AND DISCUSSION

Temperature was found to strongly influence the chemoresistive responses of the sensors. Therefore it was necessary to ensure that the temperature dependence of the sensors' output was adequately accommodated by the ANN. To test this idea, the system was subjected to the analysis of relative humidity at five levels and the temperature was allowed to vary naturally. The temperature dependence of each sensor's resistance was determined by holding the humidity constant and measuring the variation of the sensor's resistance. Fig. 4 shows how the normalized resistance, R_N , of sensor three changed as the temperature varied between 23 and 25 degrees centigrade.

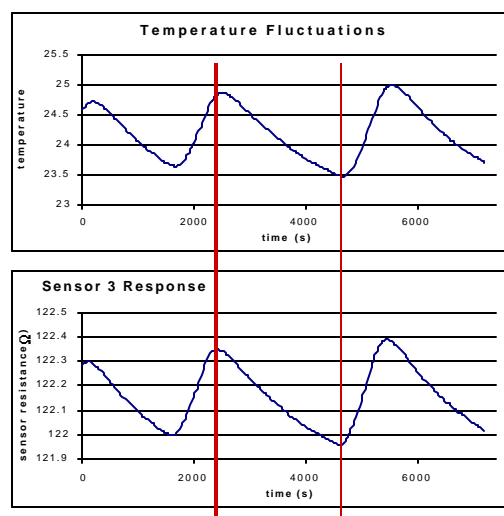


Figure 4. Typical temperature dependence of the chemoresistive VOC sensors.

The temperature coefficient of resistance, β , for each sensor was determined from the slope of the line $\ln(R_T)$ vs. $1/T$ (Fig. 3). Recognizing that the raw sensor output data contained the confounding influences of both humidity and temperature, the humidity-only responses were isolated by performing a temperature correction to the raw data. This was done by subtracting the temperature-corrected resistance from the raw measured resistance. This in effect removed the influence of the temperature dependence of the resistance of the sensor from the data. Figure 5 and Figure 6 show examples of normalized raw and temperature-corrected data of sensor element 3 in response to 30% RH respectively.

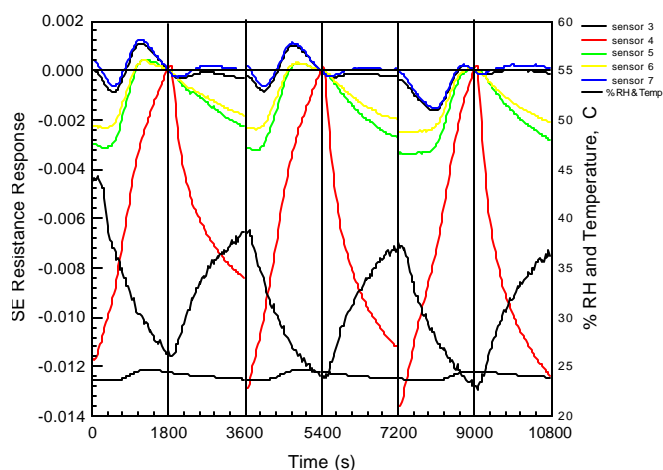


Figure 5 Normalized raw sensor data for sensor element 3.

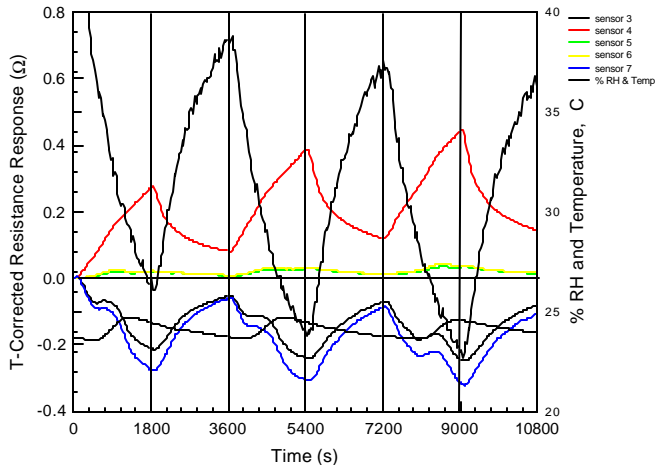


Figure 6. Normalized temperature-corrected sensor data for sensor element 3.

The ANN was trained and tested on the temperature-corrected data and conversely on the raw sensor data. The input to the ANN was a ten element input vector consisting of the 8 chemoresistive sensor responses, temperature and relative humidity. The output of the ANN was a five-element output vector where each parameter represented a specific relative humidity. The ANN was trained and tested on the temperature-corrected data using a training set size of 500 and a test set size of 50. The ANN was also separately trained and tested on the raw sensor output data using similar set sizes. Table 1 summarizes the vector outputs obtained for an unknown challenge of 36.5% RH.

10%	20%	30%	40%	50%
0.0028	0.0021	0.4297	0.5465	-0.0300

Table 1: ANN vector outputs for a 36.5% RH challenge.

The vapor concentration (RH) from the ANN output vector was determined using Equation 2.

$$\text{Calculated humidity} = \frac{\sum o_i c_i}{\sum o_i} \quad (2)$$

where o_i is the output of the i^{th} output processing element and c_i is the concentration assigned to the i^{th} output processing element.

For the above example the calculated humidity of 35.3% was obtained. The difference between the calculated humidity and the actual humidity (as measured by the internal humidity sensor) reveals an error term. This error term was used to evaluate the performance of the ANN given the two input data sets. The influence of the raw sensor data and the temperature-corrected data were compared in this way over a range of relative humidity.

The performance of the neural network was evaluated (given the two types of input data) by determining the error found between the actual humidity and the calculated humidity. The magnitude of the error was used as the basis for comparison between the two types of input data. The error obtained using raw input data was found to be 10.5% and using temperature corrected data 9.3%. This negligible difference demonstrated that the ANN was capable of adequately addressing the temperature dependence of the chemoresistive sensors. The neural network was found to successfully and accurately identify the correct RH given a vapor steam.

5 CONCLUSION

A feedforward ANN is shown to adequately address the variation in chemoresistive response that arises from confounding changes in temperature. This ability is clearly enhanced because temperature is one of the several sensor inputs passed to the ANN. This makes a strong case for the inclusion of inexpensive, mass-produced, laser-trimmed RTDs as sensory elements in various types of multi-element array electronic noses.

REFERENCES

- [1] The VCU Center for Biosensors, Bioelectronics and Biochips (CIT IO-99-010) is acknowledged for support.
- [2] (a) Farbman, A. I., "Cell Biology of Olfaction," Cambridge University Press, 79-91, 1992. (b) Kauer, J. S., Trends Neurosci. 14, 79-85, 1991.
- [3] Baltes, H, Lange D. and Koll A., IEEE Spectrum 09, 35, 1998.
- [4] Breer, H., In "Handbook of Biosensors and Electronic Noses: Medicine, Food and the Environment," Kress-Rogers, E., Ed.; CRC Press: New York, Chap. 22, 1997.
- [5] (a) Freund, M. S. and Lewis, N. S., Proc. Natl. Acad. Sci. USA 92, 2652-2656, 1995. (b) Hodgins, D. Sensors and Actuators B 27, 255-258, 1995.
- [6] Greenberg, I., "A Nose for Business," Technology Review July/August 1999, p. 63.
- [7] Menon, R., Yoon, C. O., Moses, D. and Heeger A. J., In "Handbook of Conductive Polymers," 2nd Edn., T. Skotheim, R. Elsenbaumer and J. R. Reynolds Eds.; Marcel Dekker: New York Chap. 2, pp 27 – 84, 1997.
- [8] Waldemark, J., Roppel, T., Wilson, D., Dunman, K., Padgett, M. L. and Lindblad, T., VI-DYNN 98, Stockholm June 22-26, 1998.
- [9] Gardner J W, Hines E L and Wilkinson M, Meas. Sci. Technol. 1, 446-451, 1990.
- [10] Keller, P., "Overview of Electronic Nose Algorithms" IJCNN 1999, Washington, D.C. July 1999.